ASI

Carbon – Science and Technology

ISSN 0974 – 0546

http://www.applied-science-innovations.com

RESEARCH ARTICLE Received:10/03/2016 , Accepted:24/07/2016

Numerical Investigation of Jet Impingement Heat Transfer on a Flat plate

Asem Nabadavis* **and Dipti Prasad Mishra**

Department of Mechanical Engineering, Birla Institute of Technology-Mesra, Ranchi, Jharkhand, India.

Abstract: The numerical investigation emphasizes on studying the heat transfer characteristics when a high velocity air jet impinges upon a flat plate having constant heat flux. Numerical analysis has been conducted by solving conservation equations of momentum, mass and energy with two equations based k- ε turbulence model to determine the wall temperature and Nu of the plate considering the flow to be incompressible. It was found from the investigation that the heat transfer rate increases with the increase of Reynolds number of the jet (*Rej*). It was also found that there is an optimum value for jet distance to nozzle diameter ratio (*H/d*) for maximum heat transfer when all the other parameters were kept fixed. Similar results as above were found when two jets of air were used instead of one jet keeping the mass flow rate constant. For a two jets case it was also found that heat transfer rate over the surface increases when the jets are inclined outward compared to vertical and inward jets and also there exists an optimum angle of jet for maximum heat transfer. Further investigation was carried out for different jet-to-jet separation distance for a twin jet impingement model where it was noted that heat transfer is more distributed in case of larger values of L and the rate of heat transfer increases as the separation between the jet increases till a certain point after which the rate of heat transfer decreases.

Keywords: Jet impingement heat transfer; CFD; ANSYS FLUENT.

1 Introduction: Impinging jets provide an effective and flexible way to transfer of energy in various industrial applications. A fluid flow impinged against a surface can efficiently transfer large amounts of thermal energy between the surface and the fluid. Jet impingement heat transfer can be used in metal annealing, glass annealing, paper drying, food drying, turbine blade cooling, aircraft anti-icing applications, cooling of electronic components etc.

Compared to other heat transfer arrangements that do not employ phase change, the jet impingement device offers efficient use of the fluid, and high transfer rates. When compared with conventional convection cooling by confined flow parallel to the cooled surface, jet impingement produces heat transfer coefficients that are up to three times higher at a given maximum flow speed, because the impingement boundary layers are much thinner, and often the spent flow after the impingement induces turbulence to the surrounding fluid. For a given heat transfer coefficient, the flow required from an impinging jet device is much lesser than that of cooling approach using a free wall-parallel flow.

The investigation is carried out for a hot surface having a constant heat flux of 5600 W/m^2 with air at 300 K impinging on its surface at a high velocity. In the investigation we are going to vary the ratio of jet distance to diameter of jet (*H/d*), Reynolds number of the jet (*Rej*) for single jet impingement case and inclination of the nozzle (φ) and jet-to-jet separation distance *L* are the additional parameters that are to be varied for twin jet impingement case then study the heat transfer performance characteristics.

The mass flow rate in both the cases will be kept as constant. From the investigation, we are going to predict the optimum value of the varying parameters for maximum heat transfer.

2. Literature Review: Significant experimental and numerical work has been done by several researchers to analyse the heat transfer characteristics on a surface by Jet impingement technique (JIT). Experimental study by Katti and Prabhu [1] focussed on the heat transfer enhancement from a flat surface with axisymmetric detached rib-rougheners due to normal impingement of circular air jet. Effect of rib width, rib height, pitch between the ribs, location of the first rib from the stagnation point and clearance under the rib on the local heat transfer distribution was studied. They concluded that there is a continuous enhancement in Nusselt numbers from stagnation point till the first detached rib. It may be due to fluid accelerations created in the stagnation region by the clearance under the first rib. This result is supported by lower wall static pressure under the rib, compared with smooth surface. Sagot et al. [2] experimentally investigated gas-to-wall heat transfer configuration for a round air jet impinging on a circular flat plate experimentally. These experimental measurements are compared with the results of a numerical CFD modelling to derive an average Nusselt number correlation in the jet Reynolds number range $10000 \leq Rej \leq 30\ 000$ and for various geometrical parameters $3 \leq R/D \leq 10$ and $2 \leq H/D \leq 6$. Another experimental investigation was carried out by Sagot et al. [3] on the effects of axisymmetric lathe-worked grooves on the impinging jet-to-wall heat transfer, under constant wall temperature conditions. They obtained heat transfer enhancements up to 81% for square cross-section grooves as compared with the smooth plate at $R/D = 2$, a jet Reynolds number $Rej = 23\ 000$. Bu et al. [4] experimentally investigated of the heat transfer characteristics of jet impingement on a variable-curvature concave surface in a wing leading edge was conducted for aircraft anti-icing applications. They concluded that decreasing curvature radius and increasing jet impingement angle can both enhance jet impingement heat transfer performance at the stagnation point. Fenot et al [5] investigated using A technique based on infrared thermography is used to determine the convective heat transfer on a flat plate on which either a single circular air jet or a row of jets impinged. They varied jet injection temperature, Reynolds number of jet, spacing between adjacent jet, and the distance between the flat plate and jets orifices. For all the cases, two configurations were investigated, one with semi-confinement and the other without semi-confinement. They found that the influence of confinement on heat transfer coefficient is weak, but it has a great impact on effectiveness.

Angioletti et al. [6] numerically studied by CFD turbulent modelling of heat transfer by initially laminar and transitional submerged, unconfined gaseous jet impingement on a plane target and additionally interpreted with the help of associated measurements. These measurements were validated experimentally using particle image velocimetry (PIV). Three turbulence models viz. k-ε Re-Normalized Group (RNG), k–ω Shear Stress Transport (SST) and the Reynolds Stress Model (RSM) have been enforced in the present paper, and complete velocity maps and local Nu distributions are presented and compared to the averaged or instantaneous experimental flow field and heat transfer data, verifying on the relative merits of the adopted models. They found that k–ω SST turbulence model was more reliable for the configurations, at the lower Reynolds number but for the higher Reynolds number, the comparison with the experimental data was improved by using k–ε RNG or RSM turbulence models when simulating the flow field, although all models where highly inadequate in the heat exchange valuation. Zuckerman and Lior [7] numerically investigated the heat transfer on a cylindrical surface exposed to radial impinging slot using v2f turbulence model against a published test data. The investigation yielded a correlation which can predict heat transfer on a cylindrical target over a range of parametric variables. Numerical investigation carried out by de Lima et al. [8] studied the important parameters to build a correlation that represents the compressible flow with heat transfer in internal concave curved surfaces of the aircraft wing leading edge were identified using a dimensional analysis. A functional relation was deduced so that it can be used to carry on all parameters that influence the heat transfer in impingement jets on inner surface of the aircraft wing leading edge. Afroz and Sharif [9]

numerically studied the heat transfer from an isothermally heated flat surface due to two-dimensional turbulent twin oblique confined slot-jet impingement was studied numerically using the ANSYS FLUENT. The flow and thermal fields for a normal confined slot-jet impingement are investigated using the RNG k-ε model and the SST k-ω model, and their performance was evaluated against experimental data for Re_j = 23,000 to 50,000, jet-to-jet separation distance (L = 0, 2, and 4) and the jet exit to the target plate distance (H = 2.6, 4, and 6). They found that, for jet to jet separation distance L = 2, the local Nusselt number distribution at any combination of φ, Re_j, and H, starts with a low value at the symmetry plane goes through a minimum and then a peak around the impingement location and then decreases monotonically. The peak value of the local Nusselt number decreases slightly and its location moves downstream slightly with the decrease of φ.

3. Mathematical Formulation: The computational investigation is carried out for a jet with a nozzle diameter d which impinges on the target surface having a diameter D. The nozzle distance from the target surface is H. The computational domain has a diameter of D_{CD} and a height of H_{CD} as shown in the Figure (2). The flow field in the domain is computed using two-dimensional axis-symmetry incompressible Navier–Stokes equations with a two-equation k–$\boldsymbol{\varepsilon}$ turbulence model along with the energy equation. The two equation based k–ε turbulence model is used as it is more reliable at higher Reynolds number for simulation of flow field (Angioletti et al. [5]). Air at temperature 300K is the fluid used for simulation process and the Reynolds number of the jet (Re_j) is taken as 20000 and range is H/d is $3 \leq H/d \leq 35$ for both single jet and twin jet. As the air density varies with temperature, the density of air has been computed according the ideal gas law.

3.1 Governing Equations: The governing equations for the above analysis can be written as:
Continuity equation:

$$\frac{\partial}{\partial x_i}(\rho U_i) = 0 \tag{1}$$

Momentum Equation:

$$\frac{D(\rho U_i)}{Dt} = \frac{\partial p}{\partial x_i} + \frac{\partial}{\partial x_j}\left[\mu\left(\frac{\partial U_i}{\partial x_j} + \frac{\partial U_j}{\partial x}\right) - \rho\overline{u_i u_j}\right] \tag{2}$$

where p is the modified pressure (p + 2ρk/3) and ρ is the fluid density.

$$\frac{p}{\rho} = RT \tag{3}$$

where R is the characteristic gas constant = 0.287 kJ/kg K at 300 K.

Energy equation:

$$\frac{D(\rho T)}{Dt} = \frac{\partial}{\partial x_j}\left[\left(\frac{\mu}{Pr} + \frac{\mu}{Pr_t}\right)\frac{\partial T}{\partial x_i}\right] \tag{4}$$

The density ρ is taken to be a function of temperature according to ideal gas law as per Equation (3), while dynamic viscosity μ and thermal conductivity are kept constant.

k–ε model:

Turbulence kinetic energy:

$$\frac{D(\rho k)}{Dt} = D_k + \rho P - \rho\varepsilon \tag{5}$$

Rate of dissipation of k :

$$\frac{D(\rho\varepsilon)}{Dt} = D_\varepsilon + C_{1\varepsilon}\rho P\frac{\varepsilon}{k} - C_{2\varepsilon}\rho\frac{\varepsilon^2}{k} \tag{6}$$

$$\overline{u_i u_j} = \frac{2}{3}k\delta_{ij} - \nu_t\left(\frac{\partial U_i}{\partial x_j} + \frac{\partial U_j}{\partial x_i}\right), \nu_t = 0.09\frac{k^2}{\varepsilon} \tag{7}$$

$$D_\phi = \frac{\partial}{\partial x_i}\left[\left(\mu + \frac{\mu_t}{\sigma_\phi}\right)\frac{\partial\phi}{\partial x_j}\right] \tag{8}$$

$$P = -\overline{u_i u_j}\frac{\partial U_i}{\partial x_j} \tag{9}$$

where σ_k and $\sigma_{\square}$ are Prandtl numbers for k and ε.

The constants used in the above k–ε equations are:

$C_{1\varepsilon} = 1.44$; $C_{2\varepsilon} = 1.92$; $\sigma_k = 1.0$; $\sigma_\varepsilon = 1.3$, $Pr_t = 1$.

3.2 Boundary Conditions: The boundary conditions have been shown in Figure (1) and Figure (2) for twin jet and a single jet impingement respectively. The target surface has been given a constant heat flux of 5600 W/m^2. In case of single jet, axis-symmetric boundary condition has been used whereas in case of twin jet a 3D model has been employed. Velocity inlet has been given at the nozzle exit which gives high velocity air impinging at the flat surface and the surface that is to be impinged by the jet is taken as a wall. The diameter of the jets in twin jet system has been set such that the mass flow rate of air will be the same so that a comparison between the single jet system and the twin jet system could be done. The domain limit has been treated as pressure outlet at atmospheric pressure.

$$p = p_a \tag{10}$$

In CFD simulation, the value of p_a has been taken as zero (0) as the absolute value of pressure is not important in case of an incompressible flow. The velocity at the outlet will be computed from the local pressure field so as to satisfy continuity, but all other scalar variables such as k and ε are computed from the zero-gradient condition. At the inlet, the turbulent intensity has been set to 2 percent and the turbulent viscosity ratio as 5 with the velocity known. And the backflow turbulent intensity at all the pressure outlet has been set to 5 percent but if there are no backflow at the pressure outlet then the value of k and ε are computed from the zero gradient condition at the particular point.

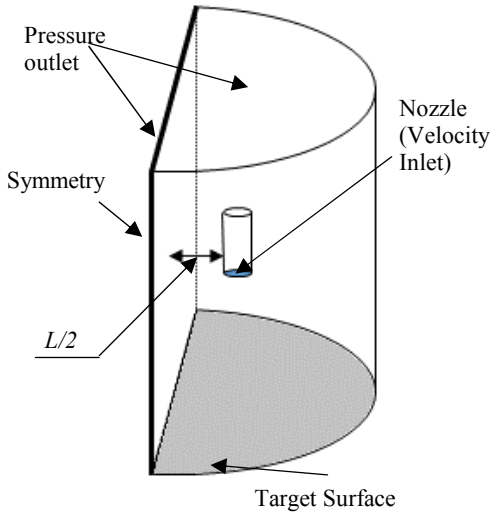

Figure (1): Computational domain of Twin Jet Impingement case.

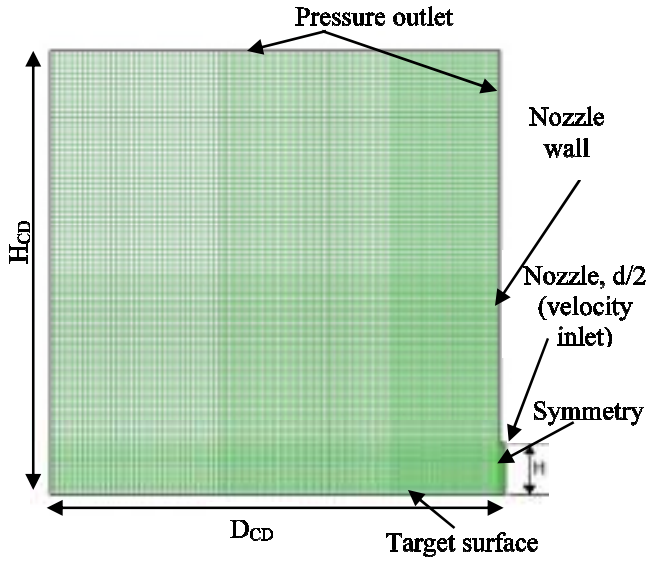

Figure (2): Computational domain of Single Jet Impingement case.

3.3 Computation of Heat Transfer and Flow Parameters: The heat transfer and flow parameters are computed as given in Bu et al. **[4]**

Local convective heat transfer coefficient,

$$h_r = \frac{q}{T_{wr} - T_{in}} \tag{11}$$

where q is the heat flux on the flat plate; T_{wx} and T_{in} are the local temperature on the plate surface and inlet temperature of supplied air respectively.

Local Nusselt number,

$$Nu_r = \frac{h_r d}{k_{air}} \tag{12}$$

where d is the diameter of nozzle and k_{air} is thermal conductivity of air.t Re_j

The jet Reynolds number,

$$Re_j = \frac{4G_m \times d}{\rho N \pi d^2 \left(\frac{\mu}{\rho}\right)} = \frac{4G_m}{N \pi d \mu} \tag{13}$$

$$G_m = \rho . \frac{\pi d^2}{4} . v_{in} \tag{14}$$

where G_m is mass flow rate of air and N is the number of jets, ρ is the density of air, μ is the viscosity of air and v_{in} is the velocity at inlet.

4 Numerical Procedure: Three-dimensional equations (two dimensional axis-symmetric for single jet) of mass, momentum, energy and turbulence have been solved, in case of multiple jet system, by the algebraic multigrid solver of Fluent 14 by using proper boundary conditions. A first order upwind scheme was considered for momentum, energy as well as turbulent discretized equations. For pressure-velocity coupling, SIMPLE (semi-implicit method for pressure-linked equation) algorithm was used for better convergence. Convergence of the discretized equations were said to have been achieved when all the residuals were below 10^{-3} for *u, v, w, p, k and* □ whereas for energy the residual level was fixed at 10^{-6}.

5 Results and Discussion:

5.1 Single Jet: For a single jet system, a two dimensional axi-symmetric model was chosen and a grid test was performed first to select the suitable grid size of the model to be simulated so that we will achieve higher order of accuracy. After the grid test simulations were done to get an optimum value for *H/d* to get maximum heat transfer. And at the end, the heat transfer characteristics were studied by varying the Reynolds number of the jet (Re_j).

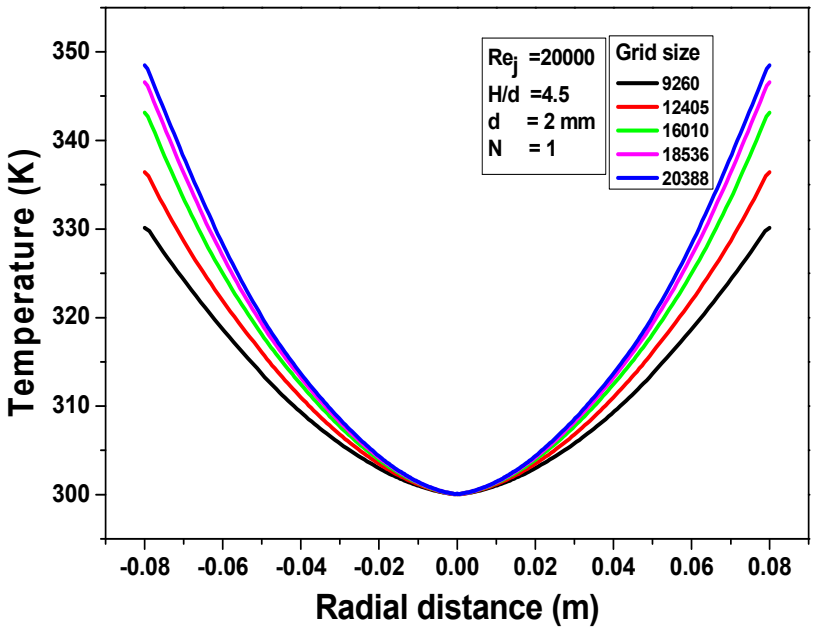

Figure (3): Grid test for single jet at Re_j=20000, H/d=4.5.

5.1.1 Grid Test: The meshing in the model was done in such a manner that the mesh was finer near the axis and wall whereas the meshes becomes coarser as we move towards the outlet. It was observed that the difference in radial temperature of plate decreases as the number of grid size increases. It was found that as the number of grids changed from 18536 to 20388 the radial temperature distribution of the plate does not vary significantly. So we have taken nearly 20000 grids to perform all the computations. However when we changed the geometry, we perform the grid test again when we report any results.

5.1.2 Variation of *H/d*: To see the effect of *H/d* on the heat transfer characteristics of jet impingement heat transfer simulations on different values of *H/d* were conducted and their characteristics were studied to predict the optimum value of *H/d* for maximum heat transfer. Observing the graphs from Figure (4), it can be concluded that the temperature of the plate does not change much beyond the value of *H/d* = 25. The local Nu distribution over the plate shows that the value of Nu for *H/d* = 25 is low initially compared *H/d* = 19 at core region, but radial outwards the *Nu* corresponding to *H/d* = 25 is more dominant. The same is also visualized in Figure (5), where the average Nusselt number was found to be highest for *H/d* = 25. When the relative tube-to-surface distance *H/d* is smaller than 25, the jet arriving at the impinging surface is not fully developed, and a potential core region exists in front of the target surface. As *H/d* decreases, the distance travelled by the jet decreases, and the shear-driven interaction between the jet and the surrounding air is limited, as a result there is drop of the local Nusselt number in the stagnation region as the jet turbulence level is decreases. For *H/d* > 25, the jet is fully developed before it impinges the plate. Under this condition, the target surface is in the downstream zone of the potential core. As the relative tube-to-surface distance increases, the distance between the nozzle and the plate increases, and the momentum and velocity in the jet core zone decreases gradually because of the shear-driven interaction between the jet and the surrounding air, as a result there is decrease of the heat transfer rate in the stagnation region of the plate [4].

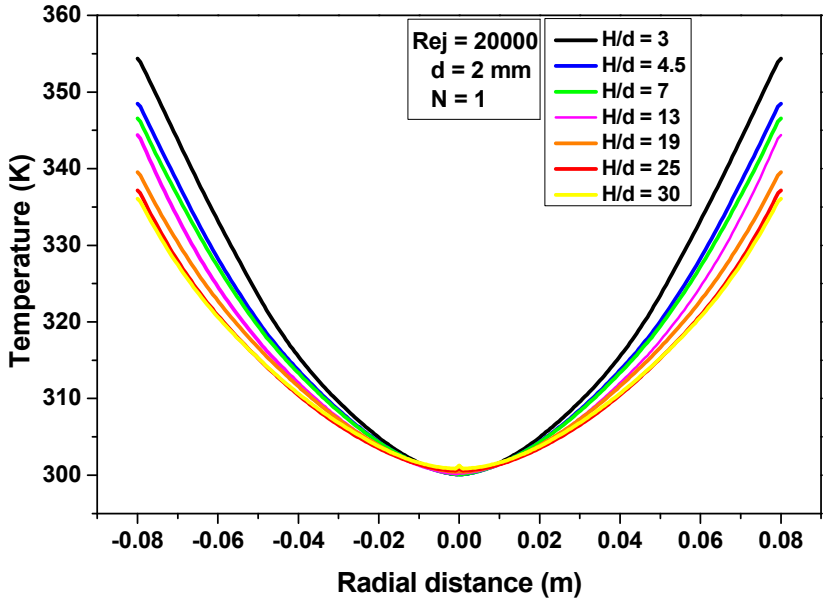

Figure (4): Temperature plot for single jet system by varying *H/d* at Re_j=20000 (3≤ *H/d* ≤ 30).

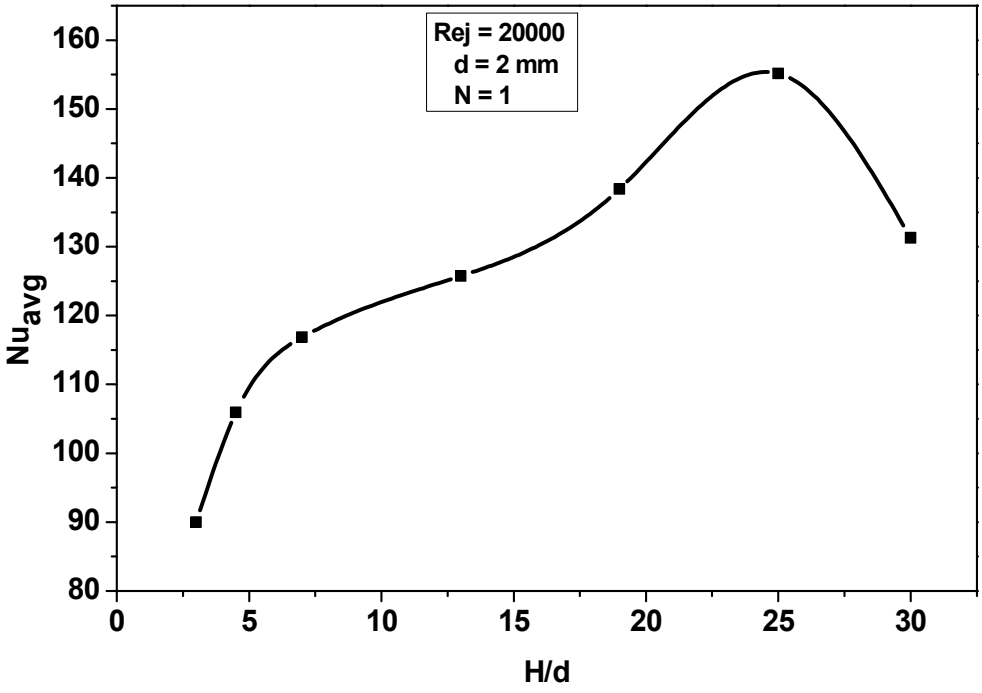

Figure (5): Average Nusselt number (Nu_{avg}) plot against H/d variation for a single jet system.

5.1.3 Variation of Re_j: The variation of jet Reynolds number has a direct effect on the heat transfer characteristics. As seen from the Figure (6), the temperature of the surface decreases as Re_j increases which in turn implies that the heat transfer rate rises as we increase Re_j. This is because when Re_j is increased the mass flow rate increases which in turn increases the mass of air in contact with the hot surface hence there is more heat transfer in the surface.

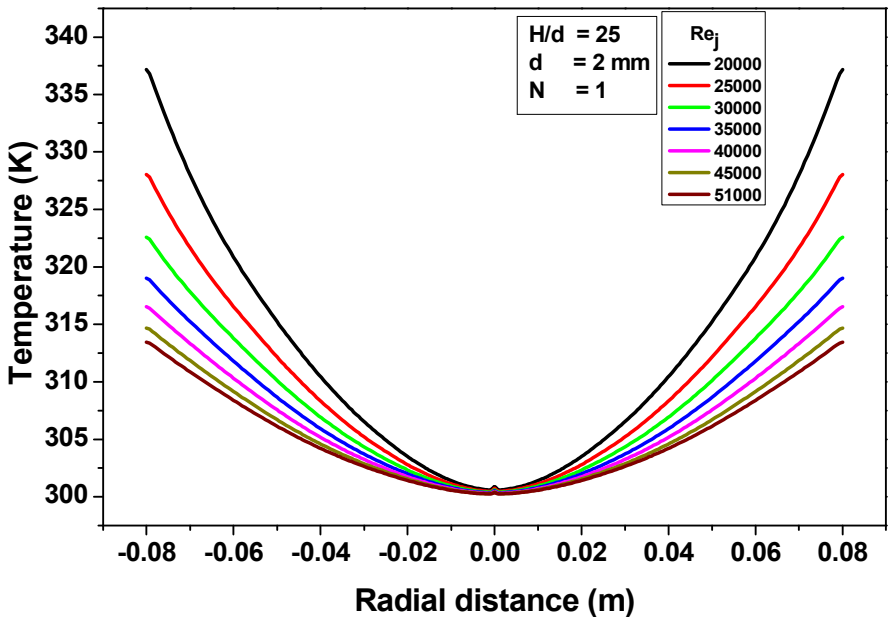

Figure (6): Temperature plot for single jet system at H/d = 25 for varying Re_j (from 20000 to 50000).

5.2 Twin Jet: For a twin jet impinging model, using a 2D model was not suitable, so 3D model have been employed by giving symmetry condition in the centre of the model. The model was considered in such a manner that the G_m (flow rate of air) will be same as in single jet impingement system. So the

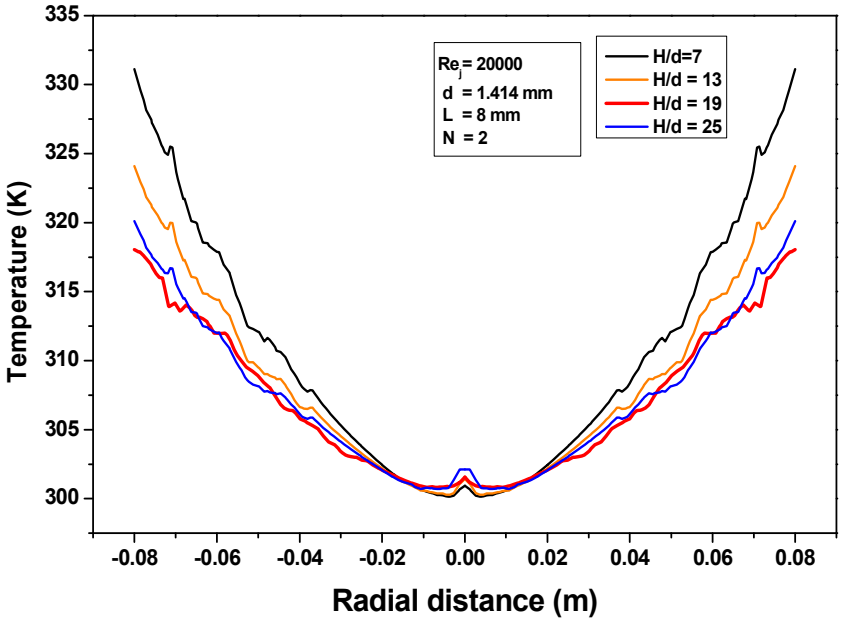

Figure (7): Temperature plot for twin jet system for varying *H/d* at Re_j=20000

diameter of jet was taken as d = 1.414 mm in case of twin jet system as there will be two jets striking on the target surface. To study the effects of twin jet, test on varying *H/d*, jet impingement angle and jet-to-jet distance were performed numerically. The results have been analyzed below.

5.2.1 Variation of *H/d*: The effect of varying *H/d* value in twin jet system will be similar to the effects in single jet system. The only difference is the value of *H/d* may not be same in both the cases. In both cases the heat transfer rate increases as the value of *H/d* increases up to a certain point then it starts decreasing. From the Figure (7) and Figure (8), it is observed that maximum heat transfer occurs at *H/d*=19.

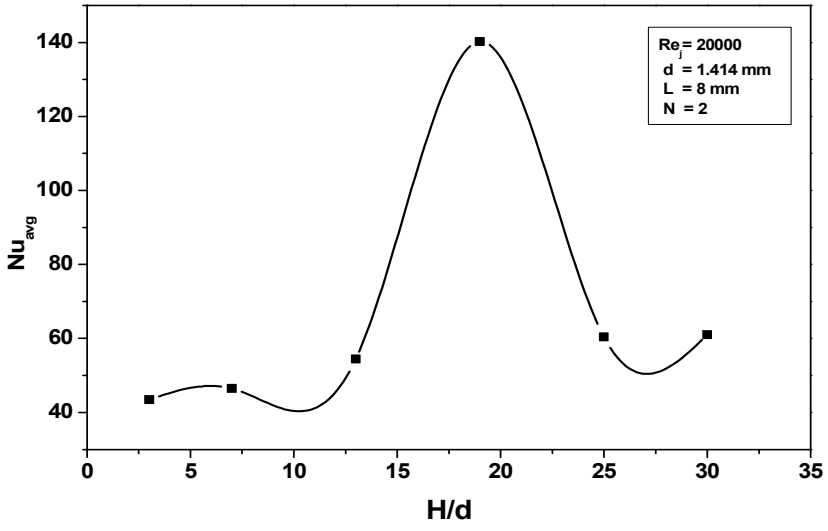

Figure (8): Nusselt number vs. *H/d* plot for twin jet system at Re_j=20000.

5.2.2 Variation of Impingement Angle, *φ*: Figure (10) shows the way in which the jet impingement angle is varied. For convenience, when the nozzle is inclined towards the symmetry φ is taken to be positive, vertical position as $\varphi = 0$ and when the nozzle is inclined outwards φ is taken to be negative. The value of φ was varied from 10^o to -30^0 at $H/d = 19$, $Re_j = 20000$ and $L = 8$mm.

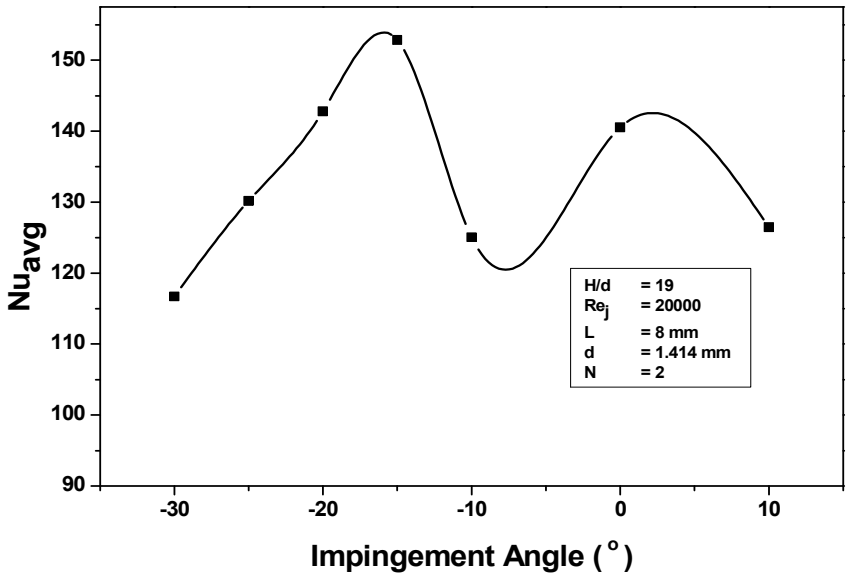

Figure (9): Average Nusselt number plot for varying impingement angle at H/d = 19, Re_j = 20000 and L = 8 mm.

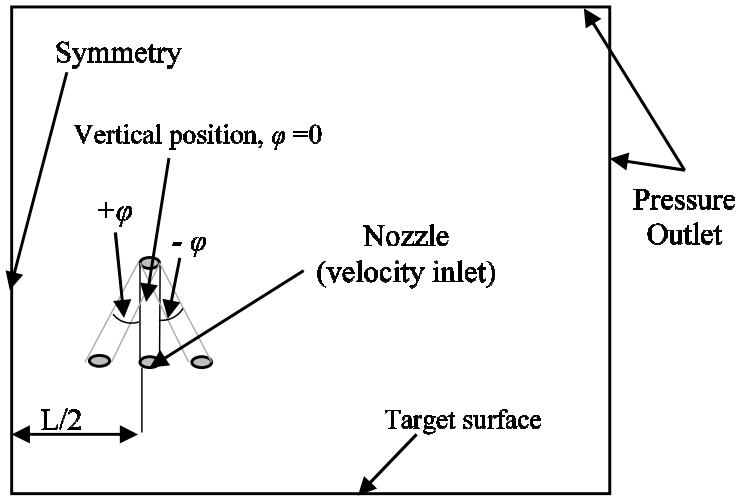

Figure (10): Schematic view of jet impingement angle variation.

When positive value of φ was taken, most of the flow was confined between the two jets and flow was getting obstructed. Thus flow does not distribute properly over the plate and the heat transfer is limited only to the central region of the plate. But when negative values of φ were taken the flow is more distributed in the entire area. As flow is more distributed in case of negative φ, rate of heat transfer will be higher. This phenomenon can be seen from the graph plotted in Figure (9). If the outward inclination of the jet is too large then the flow does not get enough contact with the plate because most of the flow will get deflected. Since it is difficult to predict which set up will have a higher rate of heat transfer, average Nusselt number has been plotted against φ. And from Figure (10), we can predict that somewhere around $\varphi = -15^o$, there is maximum heat transfer.

5.2.3 Variation of Jet-to-Jet separation distance, *L*: The effect on rate of heat transfer on a twin jet system is studied by varying the jet-to-jet distance (L) by fixing H/d at 19 and Re_j = 20000. It was observed that the average Nusselt number varies with L. At smaller values of L, heat transfer is concentrated in the region between the jets. However, at larger values of L heat transfer is more distributed. The average heat transfer rate increases as separation between the jets is increased as seen

from Figure (11) and then after reaching a peak point it drops. In this case the peak of the curve lies at L = 75 mm (Nu_{ang} is maximum at L= 75 mm). After reaching the peak, the average heat transfer decreases because the effect of flow in central region of the plate decreases and the heat transfer at central portion is greatly reduced due to this reason. Thus if the separation of the jets are too large then the rate of heat transfer will decrease rather than increase.

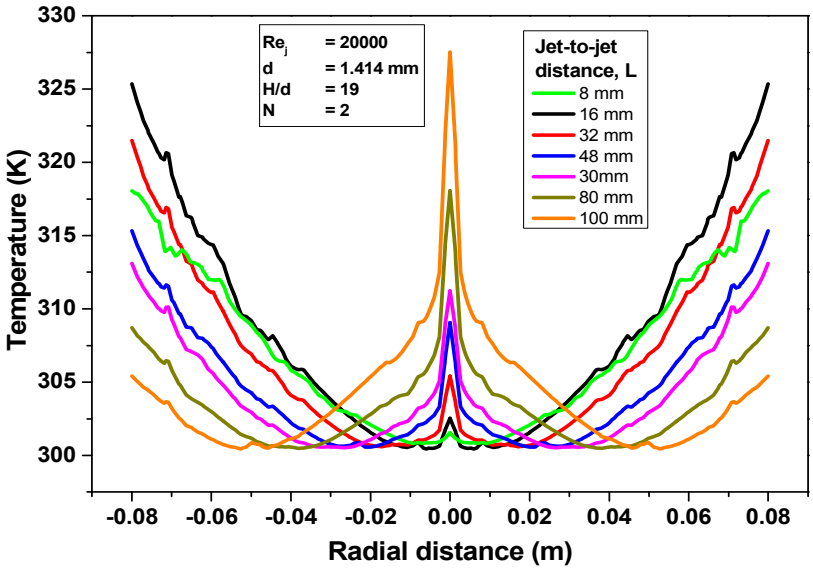

Figure (11): Temperature plot at Re_j = 20000, H/d = 19 of twin jet system for varying L.

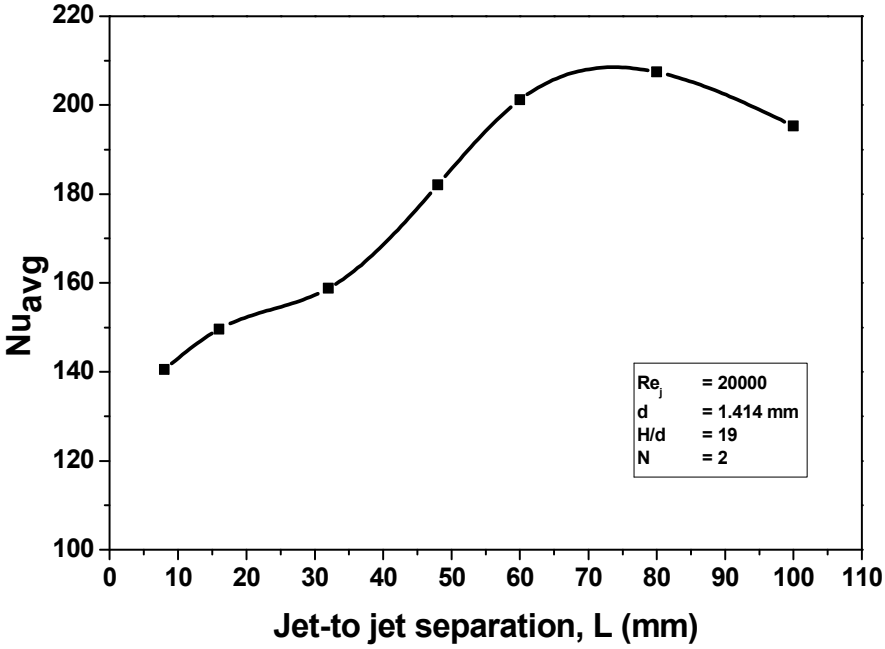

Figure (12): Average Nusselt (Nu_{avg}) number plot at Re_j = 20000, H/d = 19 of twin jet system for varying L.

6 Conclusions: In the present thesis work, configuration of single jet impingement and twin jet impingement heat transfer have been numerically analyzed using FLUENT 14. Here, a circular plate of diameter 160 mm was taken as the target surface and diameter of jet was taken as d = 2 mm (in case of single jet) and d = 1.414 mm (in case of twin jet) for the analysis.

In case of single jet, maximum heat transfer characteristic was obtained at H/d = 25 at Re_j = 20000 and it was also observed that heat transfer rate increases with the increase of Reynolds number of jet.

In case of twin jet, at Re_j = 20000 and L = 8 mm, the maximum heat transfer criteria occurs at the configuration of H/d = 19 when H/d was set as the variable. Taking this value of H/d =19 as maximum heat transfer criteria jet impingement angle, φ was varied at Re_j = 20000, L = 8 mm. Then the maximum heat transfer occurs at φ = -15°. Keeping H/d = 19 fixed, the jet-to-jet distance, L was set as variable, then it was predicted that maximum heat transfer occurs at L = 75 mm where average Nusselt number.

References:

[1] Vadiraj Katti, S. V. Prabhu, Heat transfer enhancement on a flat surface with axisymmetric detached ribs by normal impingement of circular air jet, International Journal of Heat and Fluid Flow 29 (2008) 1279–1294.

[2] B. Sagot, G. Antonini, A. Christgena, F. Buron, Jet impingement heat transfer on a flat plate at a constant wall temperature, International Journal of Thermal Sciences 47 (2008) 1610–1619.

[3] B. Sagot, G. Antonini, F. Buron, Enhancement of jet-to-wall heat transfer using axisymmetric grooved impinging plates, International Journal of Thermal Sciences 49 (2010) 1026-1030.

[4] Xueqin Bu, Long Peng, Guiping Lin, Lizhan Bai, Dongsheng Wen, Experimental study of jet impingement heat transfer on a variable-curvature concave surface in a wing leading edge, International Journal of Heat and Mass Transfer 90 (2015) 92–101.

[5] M. Fenot, J. J. Vullierme, E. Dorignac, Local heat transfer due to several configurations of circular air jets impinging on a flat plate with and without semi-confinement, International Journal of Thermal Sciences 44 (2005) 6 65–67.

[6] M. Angioletti, E. Nino, G. Ruocco, CFD turbulent modelling of jet impingement and its validation by particle image velocimetry and mass transfer measurements, International Journal of Thermal Sciences 44 (2005) 349–356.

[7] Neil Zuckerman and Noam Lior, Radial Slot Jet Impingement Flow and Heat Transfer on a Cylindrical Target, JOURNAL OF THERMOPHYSICS AND HEAT TRANSFERVol. 21, No. 3, July–September 2007.

[8] Rosiane Cristina de Lima, João Batista do Porto Neves Júnior, Edson Luiz Zaparoli, Cláudia Regina Andrade, A survey of nusselt number correlations for aircraft Thermal anti-icing design, 19th International Congress of Mechanical Engineering, November 5-9, 2007, Brasília, DF.

[9] Farhana Afroz, M.A.R. Sharif, Numerical study of heat transfer from an isothermally heated flat surface due to turbulent twin oblique confined slot-jet impingement, International Journal of Thermal Sciences 74 (2013) 1-13.

[10] H.K. Versteeg and W Malalasekera, An Introduction to Computational fluid Dynamics, The Finite Volume Method, 1995.

*****